



Landslide susceptibility assessment using analytic hierarchy process and weight of evidence methods in parts of the Rif chain (northernmost Morocco)

Abderrazzak Es-smairi¹ · Brahim El Moutchou¹ · Abdelouahed El Ouazani Touhami¹

Received: 7 February 2021 / Accepted: 16 June 2021 / Published online: 7 July 2021
© Saudi Society for Geosciences 2021

Abstract

The coastline between Tetouan and Bou Ahmed and its hinterlands, which is known for its frequency and variety of landslides at Morocco scale. In this context, the geological complexity, the steep terrain morphology, the fairly abundant rainfall, seismic activity..., etc. increase sensitivity and susceptibility to landslides. The consequences generated are extremely large on the components such as road networks, electricity networks, water lines, housing, arable land, forest areas, and coastal areas. In this study, we propose analytic hierarchy process (AHP) and weight of evidence (WofE) methods, to highlight and target potential areas vulnerable to risks of landslides to minimize the damages produced by these phenomena. Eleven parameters controlling the genesis and development of landslides in the order of priority are the following: elevation, slope, lithology, land use, rainfall, proximity to faults, proximity to streams, curvature, aspect, shaded/relief, and proximity to the road. The efficiency testing of landslide susceptibility maps showed a good precision for both AHP and WofE models by utilizing the ROC/AUC method. The comparison between validation processes indicates that WofE method is more accurate in prediction than the AHP method. The output landslide susceptibility maps can constitute a basic document for planners, managers, and regulatory bodies responsible for managing and mitigating landslide incidents at scale of area, especially with increasing housing and large projects within an unstable mountainous area.

Keywords Morocco · Landslides · Damages · Analytic hierarchy process (AHP) · Weight of evidence (WofE) · ROC/AUC method

Introduction

In recent years and at global scale in mountainous area, the occurring frequency of incidents linked to landslides has significantly increased (Pradhan and lee 2010a); they are considered one of the most threatening phenomena in many regions of the worlds (Glade and Crozier 2005; Zorn and Komac 2007; Yalcin et al. 2011; Saha et al. 2020). They are responsible for colossal damages on human life and property. The statistics of the Center for Researches on the Epidemiology of

Disasters (CRED) (Pourghasemi et al. 2012a) show that landslide occurrence is responsible for 17% of all fatalities of natural hazards worldwide whereas economic losses are in billions of dollars per year especially for USA, Japan, and the Alpine nations (Austria, France, Italy, and Switzerland) (Aleotti and Chowdhury 1999). They are ranked as the seventh most dangerous geohazards at global scale (Saha et al. 2020). This phenomenon includes all forms of terrain displacement under the effect of slope sudden variation (Flageollet 1989); it varies between debris flows up to large superficial or deep abrupt terrain detachments. Generally, the mechanism origin of landslides is rarely attributed to a single factor it attributed to a combination of several factors whether natural or anthropogenic (Varnes 1978; Crozier 1984; Iqbal et al. 2021). The main causes of terrain instability and consequently triggering landslides are lithology, structure (faults, joints), slope gradient, ground water conditions, and nature of the overburden (Agliardi et al. 2001, 2012; Dramis and Sorriso-Valvo 1994). The trend impacts related to landslide

Responsible Editor: Biswajeet Pradhan

✉ Abderrazzak Es-smairi
essmairi.a@gmail.com

¹ Geology Department Laboratory of Geology and Oceanology, (ERGO-Accreditation: UAE/E02-FS), Sciences Faculty, Abdelmalek Essaâdi University, Tétouan, Morocco

occurrence are expected to be continuously growing throughout time, for numerous reasons. For instance, increasing of regional precipitation due to climate change, continuous deforestation (agricultural lands, overgrazing, urban areas) in addition to this, the population growth leads to the booming of exploitation of mountainous areas more vulnerable to slopes failure. (Goetz et al. 2011; Regmi et al. 2014). Moroccan territory is also exposed to landslides risks, especially the Rifian domain, given its geomorphological, lithological, structural, seismic activity, and climatic characteristics, is much more affected by landslide occurrence (Millies-Lacroix 1965; El Gharbaoui 1980; Fares 1994; El kharim 2002; El moutchou 2014), and a lesser extent to the Middle Atlas as result of the strong contrast in the aforementioned characteristics. The components most exposed and damaged by landslides risks in our study area and generally at Rif scale area are the road network, the electrical and hydraulic installations, habitats and landscape of the coast and the continent, forest systems, and agricultural lands; in addition to the latter, human life is always endangered. Mapping landslide susceptibility is considered a reliable technique for landslide risk assessment, minimizing cost damages, and for a good management of hazards reduction (Guzzetti et al. 1999; Guzzetti et al. 2012; Naidu et al. 2018; Nohani et al. 2019; Biçer and Ercanoglu 2020).

The literature reviewers from different regions show wealthy approaches and methods used concerning prediction, assessment, and mapping landslide susceptibility. Heuristic, deterministic, and statistical approaches are widely experienced for the objective mentioned before (Reichenbach et al. 2018). For heuristics or qualitative approaches which are based essentially on knowledge of the terrain characteristics and the expertise of the operator who maps (Van Westen 2000), the main methods which are part of this approaches are geomorphological method (Buwal 1997; MATE/METL 1999) and the qualitative indexed heuristic method (AHP) (Pourghasemi et al. 2012b; Pourghasemi et al. 2013a; Althuwaynee et al. 2014). The deterministic approaches are based on the calculation of safety factor by using mathematical relationship and physical law (Nohani et al. 2019); it is imputable to the engineering domain. The integration of remote sensing data, GIS environment, and bivariate and multivariate statistical methods such as frequency ratio (FR) (Pradhan 2010; Pradhan and lee 2010b; Park et al. 2013; Pham et al. 2019), information value (IV) (Karim et al. 2019), weights of evidence (WoE) (Pradhan 2010; Pamela et al. 2018; Karim et al. 2019), analytic logistic regression (LR) (Pradhan and lee 2010b; Park et al. 2013; Rasyid et al. 2016; Wu et al. 2017; Saha et al. 2020), Shannon entropy (SE) (Nohani et al. 2019), evidential belief function (EBF) (Nohani et al. 2019), and fuzzy logic (Pradhan 2010, 2011; Pourghasemi et al. 2012b) constitutes an efficient tool for producing landslide susceptibility map. Lately, several machine learning and deep learning techniques have become highly demanded for many

geotechnical applications and landside identification (Zhang et al. 2015), for example, artificial neural network (ANN) (Pradhan 2010; Pradhan and Lee 2010a; Pradhan and lee 2010b; Bui et al. 2016; Saha et al. 2020; Ghorbanzadeh et al. 2019), random forest (RF) (Li et al. 2015; Saha et al. 2020), support vector machine (SVM) (Pradhan 2013; Van Den Eeckhaut et al. 2012; Bui et al. 2016; Saha et al. 2020), convolutional neural network (CNN) (Ghorbanzadeh et al. 2019), neuro-fuzzy (Pradhan 2013), decision tree (Pradhan 2013), and many others. However, of these considerable techniques, the choice of one of them in landslide susceptibility mapping is still an open topic for a debate (Guzzetti et al. 1999; Van Westen et al. 2006).

The hillslope coastline between Tetouan and Bou Ahmed and its hinterland in Rif domain is becoming more remarkable by the frequency and variety of landslide incidence. In addition to the natural factors cited before (geomorphological, lithological, structural, seismic activity and climatic) in triggering landslides, the heavy frequent rainfalls, and storms in few decades, the increase of a large building (infrastructural, residential), unplanned management, continuous deforestation for more area of agricultural, overgrazing, and urbanization would have a serious repercussions on the stability of hillslope and consequently expansion of the risks and the damages. The identification of landslide spatial distribution and determination of the type and the magnitude intervention of triggering factors is strongly recommended in the purpose to mitigate losses, select the best strategy of prevention and intervention, and control the susceptible impacts. For this reason, some attempts at landslide inventory and landslide susceptibility mapping were applied at regional or locale scale of Rif domain using various methods; as an example, we can cite geomorphological method (El Gharbaoui 1980; El Moutchou 2014), ZERMOS method (Millies-Lacroix 1965; Fares 1994), AHP (Brahim et al. 2018), WofE (Elmoulat and Ait Brahim 2018), and others.

The lack of comparative studies between heuristic techniques and bivariate models for assessment and mapping landslides occurring in Rif scale and the limitation in landslide modeling at the known factors (such as lithology, slope, hypsometry, aspect, proximity to drainage and to fault, land use) by underestimating the role of other factors, such as annual rainfall, curvature, shaded relief, and manmade activities (e.g., construction of the road network, spread of quarrying activities), constitutes one of the motivations of the current study. Thus, the main objectives of this study are the following: (i) highlighting areas most exposed to landslide occurrence at the coastline between Tetouan_Bou Ahmed and its hinterlands by using AHP and WofE techniques in GIS platform, (ii) determining the factors most significant in landslides triggering, (iii) comparing the performance of these techniques in landslide susceptibility mapping using ROC/AUC method. Nowadays, it is the first time that a landslide susceptibility assessment using analytic hierarchy process and weight of

evidence methods is applied in the coastline between Tetouan and Bou Ahmed and hinterlands. The results of this research could constitute a basic document for decision makers, future managing, and planning as well as an important literature contribution to the landslide susceptibility mapping.

Description of study area

The study area covers approximately of 1478,428 km² located in the NW part of northernmost Morocco, between 35° 20' to 35° 45' North latitude and 5° 40' to 4° 40' West longitude (Fig. 1). It is limited in the East by the Mediterranean Sea, to the West, North, and South by the limestone chain of internal Rif. Characterized by rugged mountainous area, altitude can reach 1927m in parts of the region and strong slopes are very common. The average annual rainfall is 654mm. The climate is under the combined influence of the Mediterranean and the Atlantic, a hot and dry summer, and a wet and mild winter. The study area (Fig. 1b) is a part of the Rif belt and the majority of them is an integral part of the internal Rif domain, represented by Sebtime and Ghomaride corresponding to the Paleozoic and Mesozoic sequences which affected by Alpine metamorphism during the Eocene to late Oligocene (Kornprobst 1974; Chalouan et al. 2001) and the limestone ridge a set of small nappes or scales reinforced with Triasico-Liasic carbonates

(Wildi 1983). In addition, to paleozoic tectonic klippen (sebtides, Ghomarides) and calcareous dorsal mentioned before, some extensions limited appears of domain flysch which comprising Cretaceous and Tertiary sediment and the external domain including calcareous and marly series that are made up of Mesozoic and Cenozoic. Generally, the geomorphology of the study area is represented by the high countries (the groups of the Haouz, the ridges, the headlands, and the cliffs) and the low countries (alluvium plains, sandy coasts). The area consists of six different land uses and the major part among this classification is barren land with 61% of the study area. Hydrographically, the zone areas crossed of permanent or temporary rivers with irregular regime. They are broad little encased and with great meanders in the northern part, and narrow, encased, and perpendicular to the coast in the meridional part. In addition to the active tectonic domain of the Rif, accompanied by seismic shocks resulting from the rapprochement of the Euro-Asia and the African plates, all the characteristics mentioned before make our study area a seat, which shelter several forms of instabilities.

Materials and methods

In this section, we give details of the steps and the data used during the realization of the current study. We based on

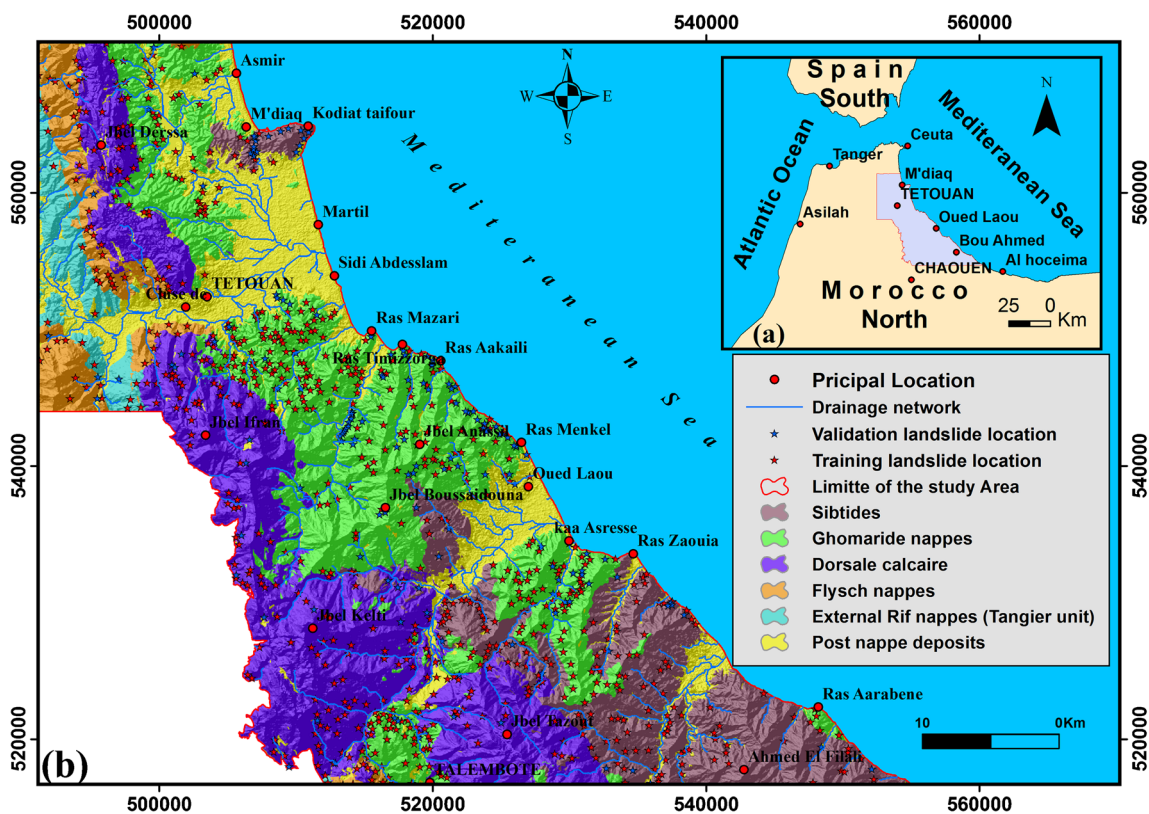


Fig. 1 a Location of the study area at the national scale. b Structural schema of the study area

several data, such as satellite, geological, topographic, and meteorological data, completing with observations of field data. The data collected were analyzed and integrated in GIS software, for generated map of landslide causative factors and the datasets for constructing and validating the models. The methods AHP and WofE were used for elaborating landslide susceptibility maps, whereas comparison and the assessment of the accuracy of them; the ROC/AUC method was employed (Fig. 2).

Inventories and mapping of landslides

The key step in the elaboration of the landslide susceptibility map is preparing an inventory map. For zoning and mapping landslides, we based on extracted data, from topographic maps, geological maps, satellite images (Landsat-8), and aerial photography. A total of 905 unstable spots with an area of 95,838 km² which corresponding to 6.482% of the total of the study area. Thereafter, the landslides inventoried were randomly divided into two groups: training data (=78%) designed for building the model and the remaining area of landslides (=22%) using for validation the model performance, which called testing data. Several types of landslides were identified (Fig. 3): rocks falls, debris flow, rotational and translational sliding, complex sliding, mudflow, and surface gullying.

Landslide causative factors

The root causes of instability of the hill slopes and consequently the occurrence of landslides in most cases is the resulting conjunction of several factors and rarely by only one. According to the several studies, determination and choice of relevant causative factors for preparing landslide susceptibility maps (LSMs) in general varies with the major characteristics of the environment context. Availability,

relevance, and practicality are the main characteristics for selected causative factors (Oh and Pradhan 2011). For elaborating LSMs, field surveys and literature review were of great importance in choice and classification of the eleven causative factors affecting the occurrence of landslides under study area which are elevation, slope, lithology, land use, rainfall, proximity to faults, proximity to streams, curvature, aspect, shaded/relief, and proximity to the roads.

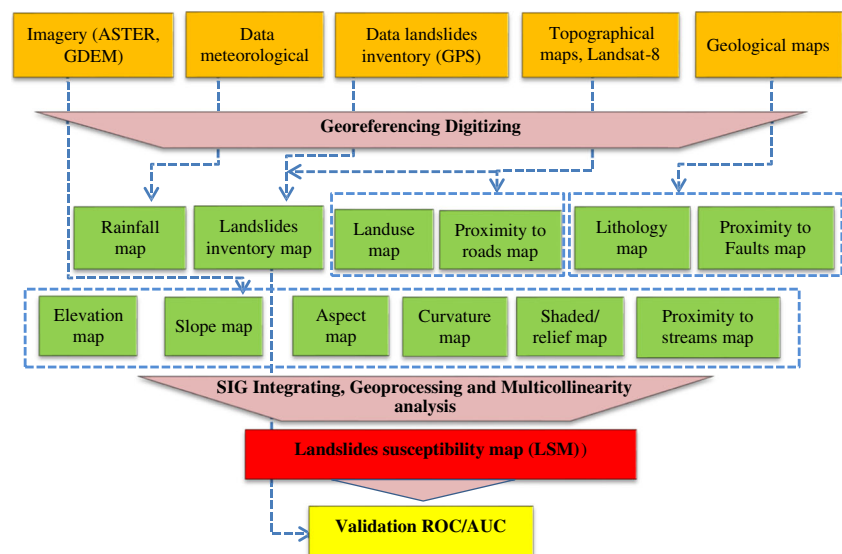
Topographic factors: elevation, slope, aspect, curvature, and shaded/relief

The geomorphological context of the study area is very fragile and constitutes a key factor in landslide genesis. Five topographic factors were selected and generated from a GDEM Aster 30m*30m.

Elevation Elevation is one of the main causal factors for slope failure; altitude influences other factors such as slope, precipitation, gravitational force, water velocity, and erosion force, which exert a strong impact at high altitude and therefore more susceptibility to landslide occurrence. The elevation map is produced and subdivided into four classes (<25m; 25–100m; 100–600m; > 600m) (Fig. 4a).

Slope The instability of the hillslope is directly dictated by the slope angle. The increase of the slope angle leads to more increasing of shear forces and consequently more instability triggering, with lithology (the degree of cohesion) and structural characteristics (faults, schistosity, fractures, diaclasses ..., etc.), constitutes determining factors in the genesis and occurrence of landslides (Van Den Eeckhaut et al. 2006; Hadji et al. 2013). The slope map produced was classified into five classes: > 2.5; 2.5–5; 5–15; 15–20; <20 (Fig. 4b).

Fig. 2 Flowchart of the methodology followed in this study



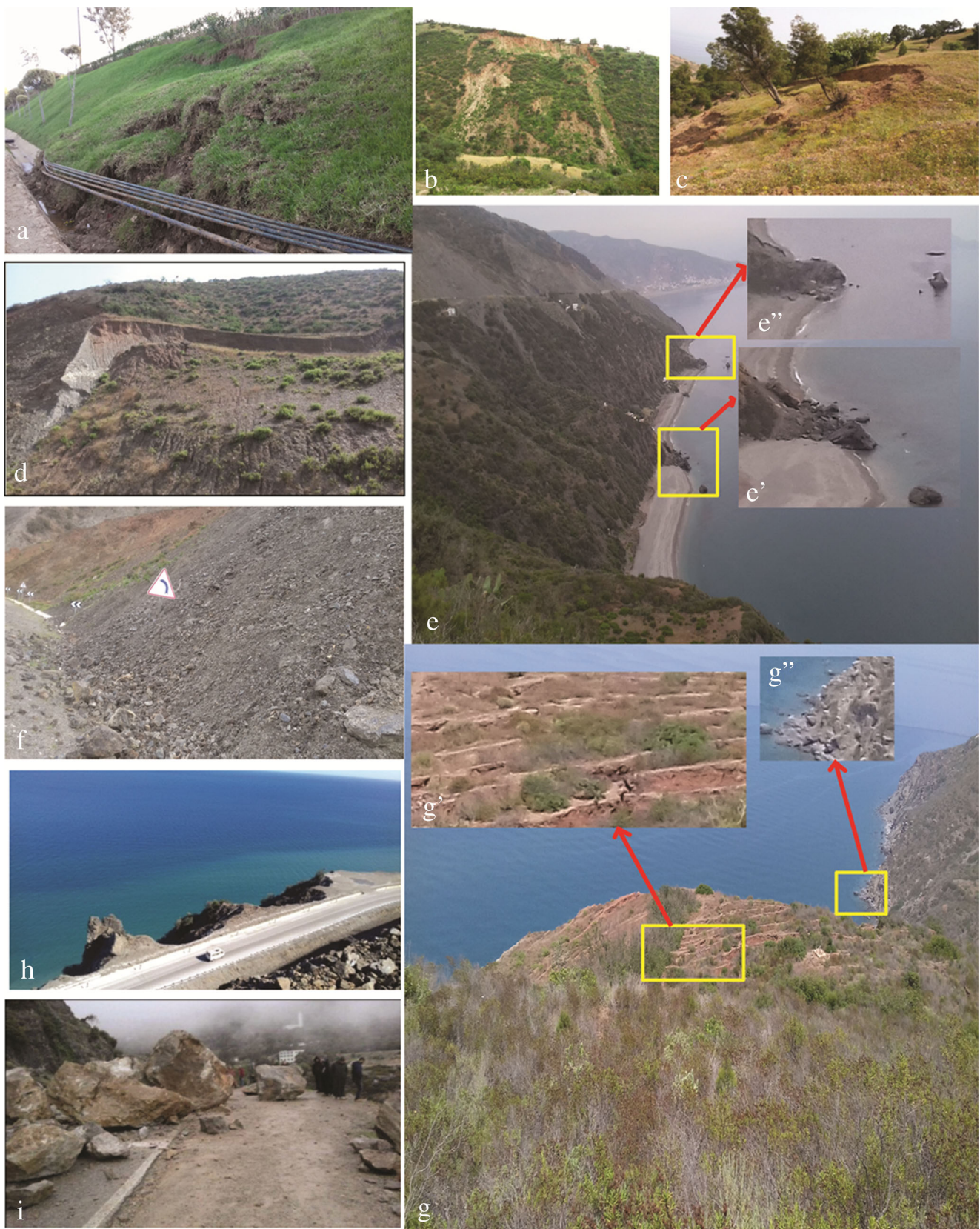


Fig. 3 Some field photos of landslides occurring in the area under study. Photographs a, c, e, f, and h show the impact of landslides on hydraulic network, agricultural lands, beaches, and road network respectively.

Photographs b, d, f, g', and i, g' translational sliding, rotational sliding, debris flow deposits, rocks fall, and complex sliding respectively

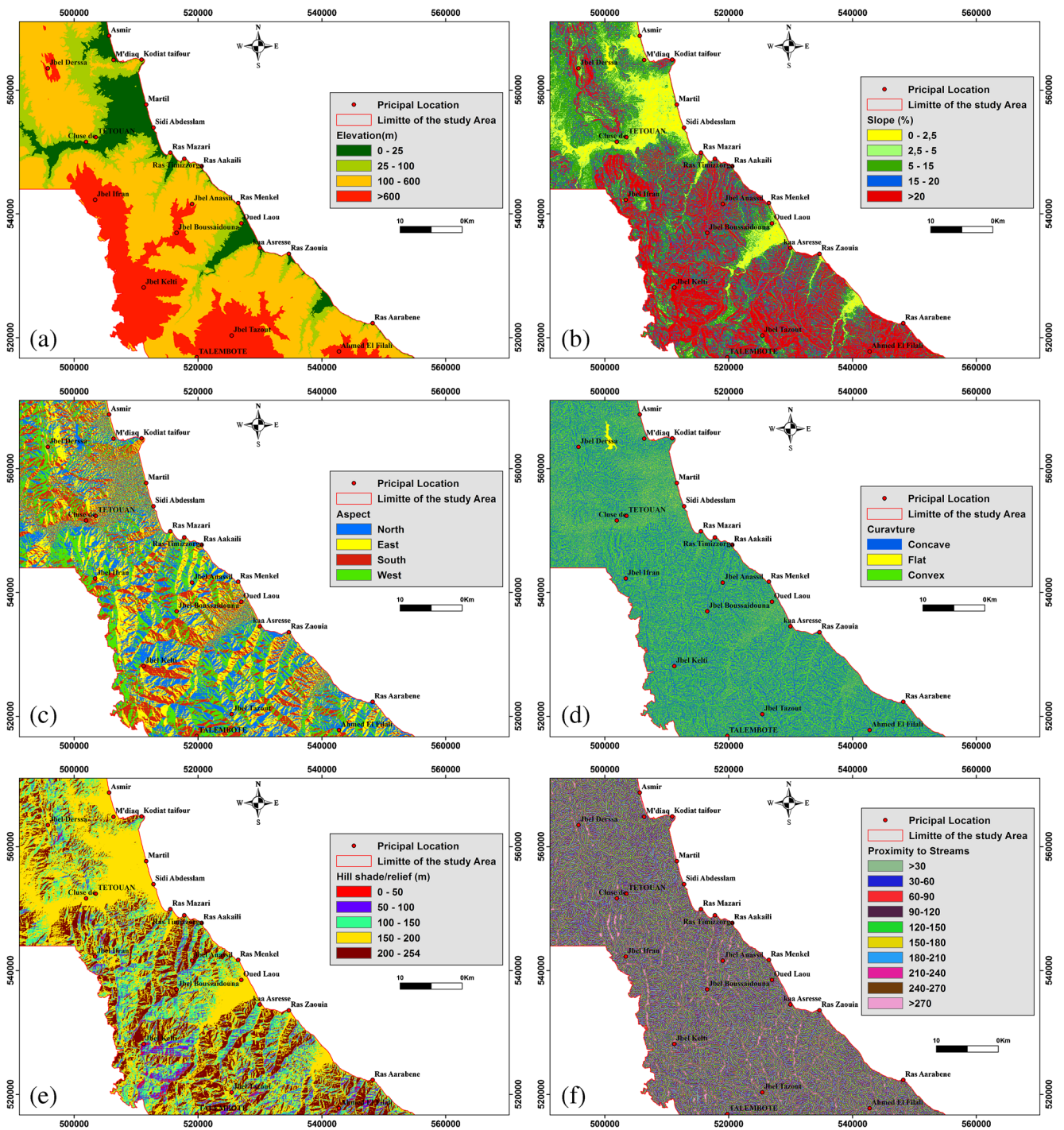


Fig. 4 a Elevation. b Slope. c Aspect. d Curvature. e Shaded relief. f Proximity to stream. g Proximity to lineaments/fault. h Proximity to roads. i Land use/cover. j Lithology. k Rainfall (mm)

Aspect The slope aspect is considered a very important factor in the genesis of landslides. It control the humidity variation of the hills slopes (Ercanoglu and Gokceoglu 2002), flow evapo-transpiration (Sidle and Ochiai 2007) and soil moisture (He et al. 2019; Jaafari et al. 2019) which lead to weak mechanical strength of rock cohesion. Four classes are determined: the

North slopes (315° – 45°), the western slopes (45° – 135°), the eastern slopes (135° – 225°), and the southern slopes (225° – 315°) (Fig. 4c).

Curvature The curvature identifies the morphology of the topography (Pourghasemi et al. 2013a). The surface of drainage

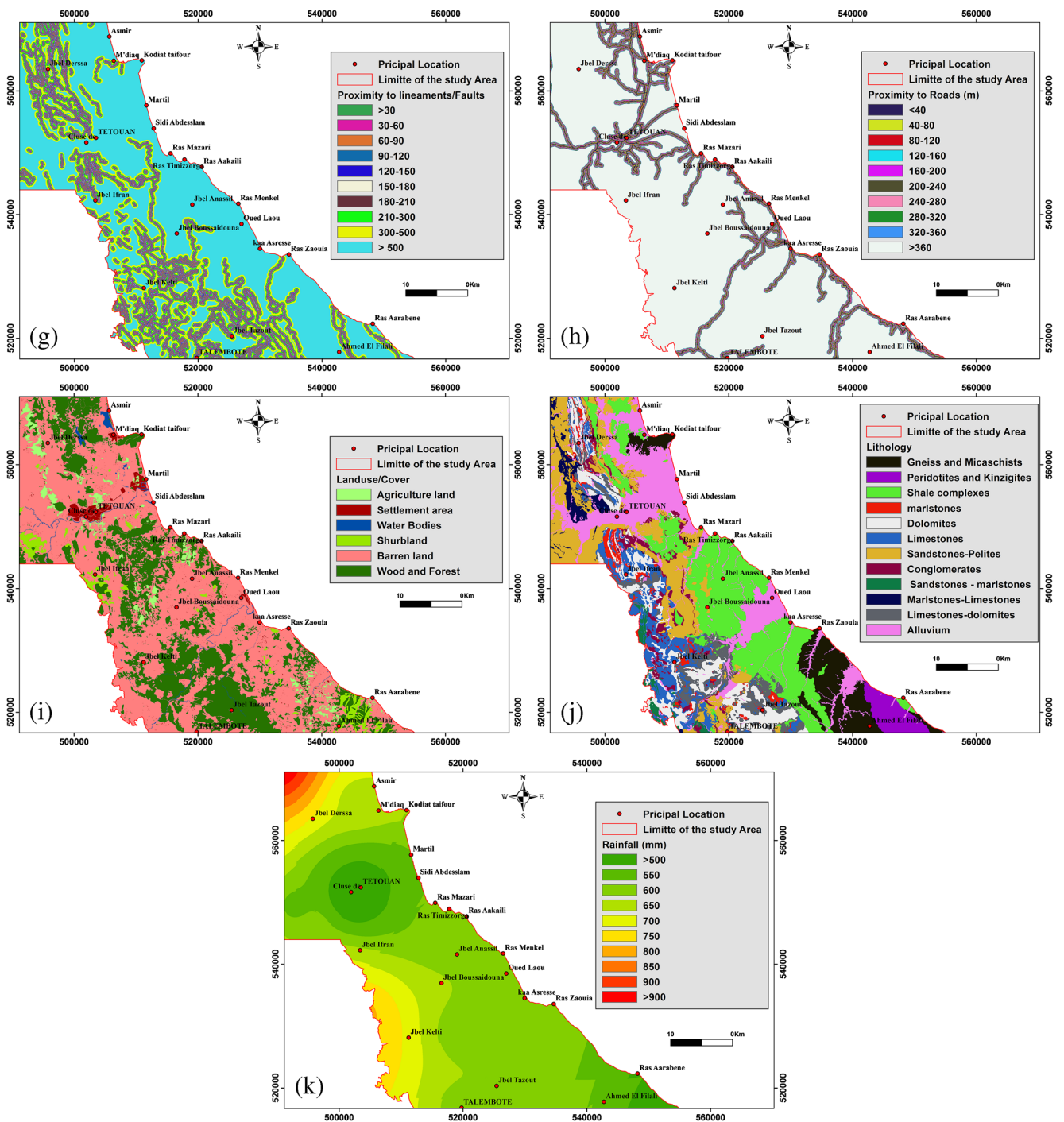


Fig. 4 (continued)

is always controlled by the curvature factor, and therefore it influences the genesis of landslides (Pham et al. 2017); after torrential rains, the regime and the flow action on the concave, flat, and convex slopes are completely different. The established map is classified into three classes: < -0.002 (concave topography); -0.002 to 0.004 (flat topography); < 0.004 (convex topography) (Fig. 4d).

Shaded relief The shaded relief parameter, or hill-shading, has been much used in cartography, to produce the illusion of a three-dimensional relief; in the literature, recently, it is used as conditioning factor in landslide occurrence (Thapa and Bhandari 2019). The shaded relief map has been established and was reclassified into 5 classes (0–50m; 50–100m; 100–150m; 150–200m; 200–254m) (Fig. 4e).

Proximity to streams

This factor acts by the erosion and the undermining of the banks of the river (Popesc 1994; Pham et al. 2018), the reason why several landslides have been mapped near the river, especially on the concave banks of the meanders where the action of water is more concentrated in particular during periods of torrential rain. The distance from river map is produced from a DEM to generate the drainage network first of all, and then calculate distance to rivers using the Euclidean distance method in a GIS, then reclassified into 10 classes (<30; 30–60; 60–90; 90–120; 120–150; 150–180; 180–210; 210–240; 240–270; > 270) (Fig. 4f).

Proximity to faults/fractures

The circulation of surface water (runoff) along the structural footprints (faults, fractures, joints, stratification) is considered a factor of destabilization of the hill's slopes. It plays a primordial role in the process of triggering landslide occurrence; the discontinuities caused in soils and rocks (Ayalew and Yamagishi 2005) make them less cohesive and less resistant (Devkota et al. 2013), promoting the circulation and infiltration of water and at the saturation threshold the landslides are triggered. The established map is produced by digitalization of the structural lineaments from the geological maps of Tetouan RasMasari, Talamboute, Bou Ahmed, and part of Beni Hassan at scale of 1/50.000, then reclassified into 10 classes (<30; 30–60; 60–90; 90–120; 120–150; 150–180; 180–210; 210–300; 300–500; > 500) (Fig. 4g).

Distance from roads

Our observations during field surveys confirm without hesitation the impact and the anthropic role in the activation and reactivation of the instabilities of the landslide occurrence in this region. The cutting of the hills for road construction, using dynamite in some place to explode hard rocks for road construction or in exploitation of quarrying, had a high impact on the stability of hill slopes and consequently activates a long process of slope instabilities difficult to control. The map is produced by digitizing the essentials of the national and regional road network based on topographic maps and the Landsat-8 satellite image of our study area, then reclassified into 10 classes: <40m; 40–80m; 80–120m; 120–160m; 160–200m; 200–240m; 240–280m; 280–320; 320–360; > 360 (Fig. 4h).

Land use/cover

Demographic expansion and the development that the region is experiencing in terms of infrastructure in recent years, lead to the more use of forest and mountain areas very susceptible

to slope failure which will undoubtedly contribute to the increasing of landslide incidence. The absence of management plans before the construction of these infrastructures amplified the landslides risks (Prokos et al. 2016). The land use map is extracted using the digitalization of topographic maps (Tetouan, Ras Mazari, Talembote, Bou Ahmed, and part of Beni Hessane at the scale of 1/50.000) coupled with the supervised classification of the Landsat-8 satellite imagery, using the maximum likelihood method. Six classes have been identified: water bodies; barren land; sparsely vegetated; agriculture land; settlement area; wood and forest (Fig. 4i).

Lithology

Geotechnical and geomechanical properties of the rocks and soil with other factors (such as faults, fractures, elevation, slope, precipitation, etc.), this factor becomes relevant in the process of instability of hill slope and landslide occurrence. To produce lithological map, we have digitized the geological maps of Tetouan RasMasari, Talamboute, Bou Ahmed, and part of Beni Hassan at scale of 1/50.000, and then reclassified on GIS according to the geotechnical and geomorphological affinities; 12 classes were identified (gneiss and mica schists; peridotites and kinzigites; shale complex; marlstones; limestone dolomites; sandstone-pelite, conglomerates, sandstones-marlstones, marlstones-limestone, limestones-dolomites; alluvium (Fig. 4j)).

Rainfall map

The abundance of rainfall is a very crucial factor in the occurrence of landslides, especially in rainy periods. Indeed, the water saturation of the soil increases the pore pressure and decreases the cohesion forces and the shear strength thus triggering instabilities (Song et al. 2012; Hamed et al. 2014). To characterize the spatial variations of the pluviometry, we use the data of the annual average precipitations between the periods (1936–2017), of stations located in our study area and those neighboring. By the interpolation method, a spatial distribution map of rainfall is produced and reclassified into 10 classes (> 500mm; 500–550mm; 550–600mm; 600–650mm; 650–700mm; 700–750mm; 750–800mm; 800–850mm; 850–900mm; > 900mm) (Fig. 4k).

Landslide susceptibility analyses

Weight of evidence method

The susceptibility to landslides has been established by a quantitative method using theory of evidence. It is a bivariate method based on the Bayesian probabilistic method (Van Westen 2000). For running the model, we were based on Eq. (1) and Eq. (2) which correspond to weight positive

(W^+) and weight negative (W^-), respectively (Regmi et al. 2010; Pradhan 2010); the weights of each causative factor (N) class are estimated based on the presence or absence of landslide occurrence within factor class (Pradhan 2010).

$$W^+ = \ln\left(P\left(\frac{M}{N}\right) \middle| P\left(\frac{M}{N}\right)\right) \tag{1}$$

$$W^- = \ln\left(P\left(\frac{\bar{M}}{N}\right) \middle| P\left(\frac{\bar{M}}{N}\right)\right) \tag{2}$$

where P is the probability and \ln is the natural logarithm; M and \bar{M} are the presence or absence of landslide causative factors; N and \bar{N} are the presence or absence of landslide occurrence, respectively. W^+ and W^- are the weights of presence or absence of landslides. The variation from W^+ to W^- corresponds to weight contrast C .

$$C = W^+ - W^- \tag{3}$$

Analytic hierarchy process (AHP)

In this study, analytic hierarchy process (AHP) was used for landslide susceptibility analyses. Saaty (1980) proposed this method for classifying a problem into different hierarchy level. In order to calculate the weights of each causative factors, firstly, all the significant predictive landslide causative factors (elevation, slope, lithology, land use, rainfall, proximity to faults, proximity to streams, curvature, aspect, shaded/relief, proximity to the road) were reorganized in a hierarchical order; secondly, based on our field knowledge and according to the importance of them in landslide process, we created the AHP matrix by a dual comparison between all factors in

pairwise comparison (Table 1), which used as the input values in the AHP matrix, which then normalized and standardized for determining the CR of the matrix. If CR is less than 0.1, the model AHP is acceptable and it discarded if CR is greater than 0.1. After calculating the weight of each causative factor, we assigned for each classes factor a weight based on the percentage of inventoried landslides within this classes.

$$CR = \frac{CI}{RI} \tag{4}$$

where

$$CI = \frac{\lambda_{max} - 1}{n - 1} \tag{5}$$

where CR and CI correspond to consistency ratio and consistency index, respectively. RI is the random index that depends on the number of causative factors, λ_{max} is principal eigenvalue in the matrix, and n is the number of causative factors.

Results

Multicollinearity diagnosis

In this study, in order to avoid no collinearity between the selected causative factors for landslide susceptibility mapping, a multicollinearity test was applied by calculating variance inflation factors (VIF) and tolerances method. According to Pourghasemi et al. (2012a), the values of $VIF > 10$ or tolerance < 0.1 stated a problem of multicollinearity of causative factors. The results of the test (Table 2) confirm all factors used were independent between each other.

Table 1 Pairwise comparison matrix

Factors	1	2	3	4	5	6	7	8	9	10	11
1	1.00										
2	0.50	1.00									
3	0.50	1.00	1.00								
4	0.25	0.33	0.50	1.00							
5	0.33	0.33	0.50	0.50	1.00						
6	0.20	0.20	0.20	0.25	0.25	1.00					
7	0.50	0.50	0.50	0.50	1.00	1.00	1.00				
8	0.20	0.20	0.20	0.25	0.25	0.25	0.25	1.00			
9	0.25	0.25	0.25	0.25	0.25	0.25	0.33	0.33	1.00		
10	0.14	0.14	0.20	0.20	0.25	0.25	0.33	0.33	0.33	1.00	
11	0.11	0.11	0.11	0.13	0.13	0.13	0.14	0.17	0.20	0.11	1.00
Wight factors	0.218	0.169	0.150	0.112	0.093	0.066	0.083	0.042	0.037	0.025	0.012

1, elevation; 2, slope; 3, lithology; 4, land use; 5, rainfall; 6, fault proximity; 7, stream proximity; 8, curvature; 9, aspect; 10, shaded/relief; 11 proximity to roads

Table 2 Indices of multicollinearity diagnosis for landslide causative factors

Model	Collinearity statistics	
	Tolerance	VIF
Altitude	0.195	5.141
Slop	0.220	4.552
Aspect	0.991	1.009
Curvature	0.983	1.017
Shaded	0.969	1.032
Proximity to stream	0.971	1.03
Proximity to fault	0.712	1.404
Proximity to road	0.903	1.108
Land use	0.904	1.106
Lithologies	0.391	2.557
Rainfall	0.832	1.201

Landslide susceptibility map using WofE model

The analysis of the results of Table 2 showed that all causative factors used in the modeling in both WofE and AHP methods were contributed in landslide process occurring whether with a weak or strong weight value. These findings go with the results of other researches (Varnes 1978; Crozier 1984), which stated that landslides are the result of conjugation for more than only factor.

As shown in Table 3, the weights obtained using WofE model for each classes of causative factors represent the impact magnitude for those classes in landslide events. Thus, a weak magnitude or negative value of weight contrast of a class is corresponding to the no significant correlation of this later in landslide occurrence. For elevation impact, the 2 first (<25m, 25–100m) classes and the last class (600–1926m) had very small impact on the landslides under the study area; the elevation between 100 and 600m had the greatest impact on landslides. Regarding the slope angle influence, the classes of 5°–10° and 10°–15 are corresponding to the most prone areas to landslide occurrence, respectively. The remaining classes (<5° and >20) show a weak probability of landslide occurrence. Under the study area, the North direction followed by the West direction had the most influence on landslide occurrence against the other directions (South and East). Among the curvature classes, landslides preferentially occur near concave slope than the other classes (flat, convex). Concerning hill shaded influence, the 200–254m class had the largest impact on landslide occurrences than the remaining classes. For the distance from streams indicating a rational correlation with landslide occurrence, thus the first 3 classes (<30, 30–60, and 60–90m) were the most unstable areas to prone landslides.

For distance from faults, the most influenced classes were in the distance range between 90 to 500m from faults. For distance from roads, the effective class was 280–320m. The barren land is one of the most components exposed to landslide occurrence of all remaining classes of land-use cover. In the case of lithology impact, the analyses of results of Table 3 showed that among all lithology units, sandstones-marlstones, marlstones-limestones, and sandstones-pelites had the greatest probability to landslide occurrence. The other units (alluvium, peridotites and kinzigites, gneiss and mica schists, shale complex) have a lower probability to landslide occurrence. Rainfall is another relevant factor in landslides triggering especially in heavy rainfalls; it leads to the surface gully and the bursting of the rock soils due to water saturation, which reduces the cohesion and resistance of the hill slopes; the classes that show the greatest impact in triggering landslides are 700–750mm and 750–800mm, respectively. Equation (6) was used in GIS to elaborate LSM (Fig. 5a). The obtained map was classified into five susceptibility classes using natural break method (Pourghasemi et al. 2012a). Percent areas of the susceptibility classes of very low, low, moderate, high, and very high were 9.740, 7.932, 25.321, 36.203, and 20.804, respectively (Fig. 6a).

$$\begin{aligned}
 \text{LSM}_{\text{WofE}} = & \text{WofE}_{\text{elevation}} + \text{WofE}_{\text{slope}} + \text{WofE}_{\text{aspect}} \\
 & + \text{WofE}_{\text{curvature}} + \text{WofE}_{\text{shaded/relief}} \\
 & + \text{WofE}_{\text{proximity to stream}} + \text{WofE}_{\text{proximity to faults}} \\
 & + \text{WofE}_{\text{proximity to roads}} + \text{WofE}_{\text{land use}} \\
 & + \text{WofE}_{\text{lithology}} + \text{WofE}_{\text{Rainfall}} \quad (6)
 \end{aligned}$$

Landslide susceptibility map using AHP method

The landslide susceptibility map (LSM) (Fig. 5b) was prepared based on Eq. (7) proposed by Voogd (1983). Using natural break method, the susceptibility values of the map prepared were classified into five classes very low, low, moderate, high, and very high which cover of the study area, 9.710, 7.882, 24.598, 34.335, and 23.475 respectively (Fig. 6b). The results of the weight score of each factor involved in the triggering of landslides are exhibited in Table 3. In this study, elevation, slope, lithology, land use, and rainfall, respectively, weighting 0.218, 0.169, 0.150, 0.112, and 0.093 are found to be determined factors on stability of hill slope and consequently in triggering landslide occurrence in our study area, whereas the remaining factors (fault proximity, stream proximity, curvature, aspect, shaded relief, road proximity) were less implicated in the process of triggering landslide occurrence according to this method.

Table 3 Spatial relationship between each landslide causative factors and occurring landslides using weight of evidence (WofE) and analytic hierarchy process (AHP) models

	Numbers of pixels	Percent of pixels	Landslide numbers	Percent of landslides	Weight of evidence			AHP		
					W ⁺	W ⁻	C	Index	Weight	
Factors										
Elevation (m)										
0–25	201,643	10.69	1575	1.66	-0.828	0.044	-0.872	1	0.218	
25–100	264,516	14.023	12,245	12.905	-0.041	0.006	-0.047	7		
100–600	954,718	50.614	60,171	63.415	0.089	-0.121	0.210	9		
600–1926	465,400	24.673	20,894	22.02	-0.057	0.018	-0.074	6		
Slope (°)										
0_2.5	164,427	8.717	1284	1.353	-0.828	0.036	-0.864	1	0.169	
2.5_5	127,393	6.754	3401	3.584	-0.287	0.015	-0.302	1		
5_15	558,690	29.619	38,018	40.067	0.130	-0.069	0.199	6		
15_20	332,397	17.622	18,557	19.557	0.043	-0.010	0.053	8		
20_73	703,370	37.289	33,625	35.438	-0.031	0.018	-0.050	9		
Aspect										
N	518,452	27.485	29,648	31.246	0.052	-0.022	0.073	9	0.037	
E	519,854	27.56	26,260	27.676	-0.004	0.002	-0.006	4		
S	399,591	21.184	14,690	15.482	-0.146	0.033	-0.179	1		
O	448,380	23.771	24,287	25.596	0.028	-0.009	0.037	8		
Curvature										
Concave	872,423	46.251	48,319	50.924	0.032	-0.031	0.063	8	0.042	
Flat	149,588	7.93	7433	7.834	-0.007	0.001	-0.008	2		
Convex	864,266	45.819	39,133	41.243	-0.058	0.046	-0.103	1		
Hill shade/relief (m)										
0–50	24,882	1.319	843	0.888	-0.179	0.002	-0.181	3	0.025	
50–100	120,178	6.371	4324	4.557	-0.153	0.009	-0.162	5		
100–150	369,378	19.582	17,272	18.203	-0.038	0.009	-0.046	6		
150–200	908,220	48.149	42,994	45.312	-0.038	0.034	-0.073	8		
200–254	463,619	24.579	29,452	31.04	0.100	-0.039	0.139	9		
>254										
Proximity to streams (m)										
<30	376,524	19.961	24,507	25.828	0.113	-0.033	0.146	9	0.083	
30–60	335,536	17.788	21,010	22.143	0.096	-0.024	0.119	9		
60–90	297,363	15.765	16,960	17.874	0.054	-0.011	0.064	8		
90–120	255,113	13.525	12,606	13.286	-0.011	0.002	-0.013	7		
90–150	208,257	11.041	8617	9.082	-0.091	0.010	-0.101	6		
150–180	155,961	8.268	5257	5.54	-0.183	0.014	-0.196	5		
180–210	109,286	5.794	2930	3.088	-0.285	0.013	-0.298	4		
210–240	71,085	3.769	1594	1.68	-0.364	0.010	-0.374	2		
240–270	41,651	2.208	787	0.829	-0.440	0.006	-0.446	2		
>270	35,501	1.882	617	0.65	-0.476	0.006	-0.482	1		
Proximity to faults (m)										
<30	75,920	4.025	1258	1.326	-0.498	0.013	-0.510	9		0.066
30–60	74,365	3.942	2492	2.626	-0.185	0.006	-0.191	9		
60–90	71,041	3.766	3611	3.806	0.004	0.000	0.004	9		
90–120	67,641	3.586	4279	4.51	0.104	-0.004	0.109	9		
120–150	64,601	3.425	4542	4.787	0.154	-0.006	0.160	8		
150–180	60,951	3.231	4589	4.836	0.186	-0.008	0.193	8		
180–210	57,478	3.047	4318	4.551	0.185	-0.007	0.192	8		
210–300	153,926	8.16	11,568	12.192	0.183	-0.020	0.203	5		
300–500	256,283	13.587	18,236	19.219	0.156	-0.030	0.186	5		

Table 3 (continued)

	Numbers of pixels	Percent of pixels	Landslide numbers	Percent of landslides	Weight of evidence			AHP	
					W^+	W^-	C	Index	Weight
>500	1,004,071	53.23	39,992	42.148	-0.116	0.110	-0.226	1	
Proximity to roads (m)									
<40	65,808	3.489	2594	2.734	-0.111	0.004	-0.115	9	0.012
40–80	46,208	2.45	1816	1.914	-0.113	0.003	-0.115	9	
80–120	43,611	2.312	1827	1.925	-0.084	0.002	-0.086	8	
120–160	41,418	2.196	1659	1.748	-0.104	0.002	-0.106	8	
160–200	39,292	2.083	1682	1.773	-0.074	0.001	-0.075	7	
200–240	37,340	1.98	1731	1.824	-0.038	0.001	-0.038	7	
240–280	35,663	1.891	1760	1.855	-0.009	0.000	-0.009	6	
280–320	33,739	1.789	1711	1.803	0.003	0.000	0.003	6	
320–360	32,434	1.719	1602	1.688	-0.009	0.000	-0.009	5	
>360	1,510,764	80.092	78,503	82.735	-0.005	0.023	-0.027	1	
Land-use/cover									
Water bodies	16,270	0.863	223	0.235	-0.581	0.003	-0.584	3	0.112
Barren land	1,158,850	61.436	63,771	67.209	0.025	-0.048	0.073	9	
Shrubland and sparsely vegetated	53,609	2.842	1756	1.851	-0.195	0.005	-0.199	1	
Agriculture land	61,195	3.244	2779	2.929	-0.047	0.002	-0.049	6	
Settlement area	31,073	1.647	1458	1.537	-0.032	0.001	-0.033	4	
Wood and forest	565,280	29.968	24,898	26.24	-0.067	0.026	-0.093	3	
Lithology									
Gneiss and mica schists	156,561	8.3	4987	5.256	-0.208	0.015	-0.223	3	0.150
Peridotites and kinzigites	55,225	2.928	749	0.789	-0.586	0.010	-0.596	2	
Shale complex	417,931	22.156	19,560	20.614	-0.038	0.010	-0.048	5	
Marlstones	41,020	2.175	1936	2.04	-0.030	0.001	-0.030	6	
Dolomite	181,724	9.634	9952	10.488	0.037	-0.004	0.041	6	
Limestone	146,268	7.754	8056	8.49	0.040	-0.003	0.043	6	
Sandstone-pelite	299,362	15.871	27,121	28.583	0.268	-0.073	0.341	8	
Conglomerates	61,635	3.268	3990	4.205	0.115	-0.004	0.120	7	
Sandstones-marlstones	19,406	1.029	2796	2.947	0.501	-0.009	0.510	9	
Marlstones-limestone	43,379	2.3	5492	5.788	0.436	-0.017	0.452	9	
Limestone-dolomite	123,641	6.555	7562	7.97	0.088	-0.007	0.095	7	
Alluvium	340,125	18.032	2684	2.829	-0.824	0.078	-0.902	1	
Rainfall (mm)									
<500	0	0	0	0	0.000	0.000	0.000	4	0.093
500–550	104	0.006	0	0	0.000	0.000	0.000	4	
550–600	26,524	1.406	661	0.697	-0.317	0.003	-0.320	4	
600–650	144,742	7.673	6644	7.002	-0.043	0.003	-0.047	5	
650–700	789,042	41.831	37,855	39.896	-0.031	0.022	-0.053	5	
700–750	691,076	36.637	36,686	38.664	0.016	-0.010	0.025	6	
750–800	161,945	8.585	10,788	11.37	0.127	-0.014	0.141	9	
800–850	35,891	1.903	1594	1.68	-0.057	0.001	-0.058	7	
850–900	14,564	0.772	359	0.378	-0.321	0.002	-0.323	7	
<900	22,389	1.187	298	0.314	-0.594	0.004	-0.598	8	

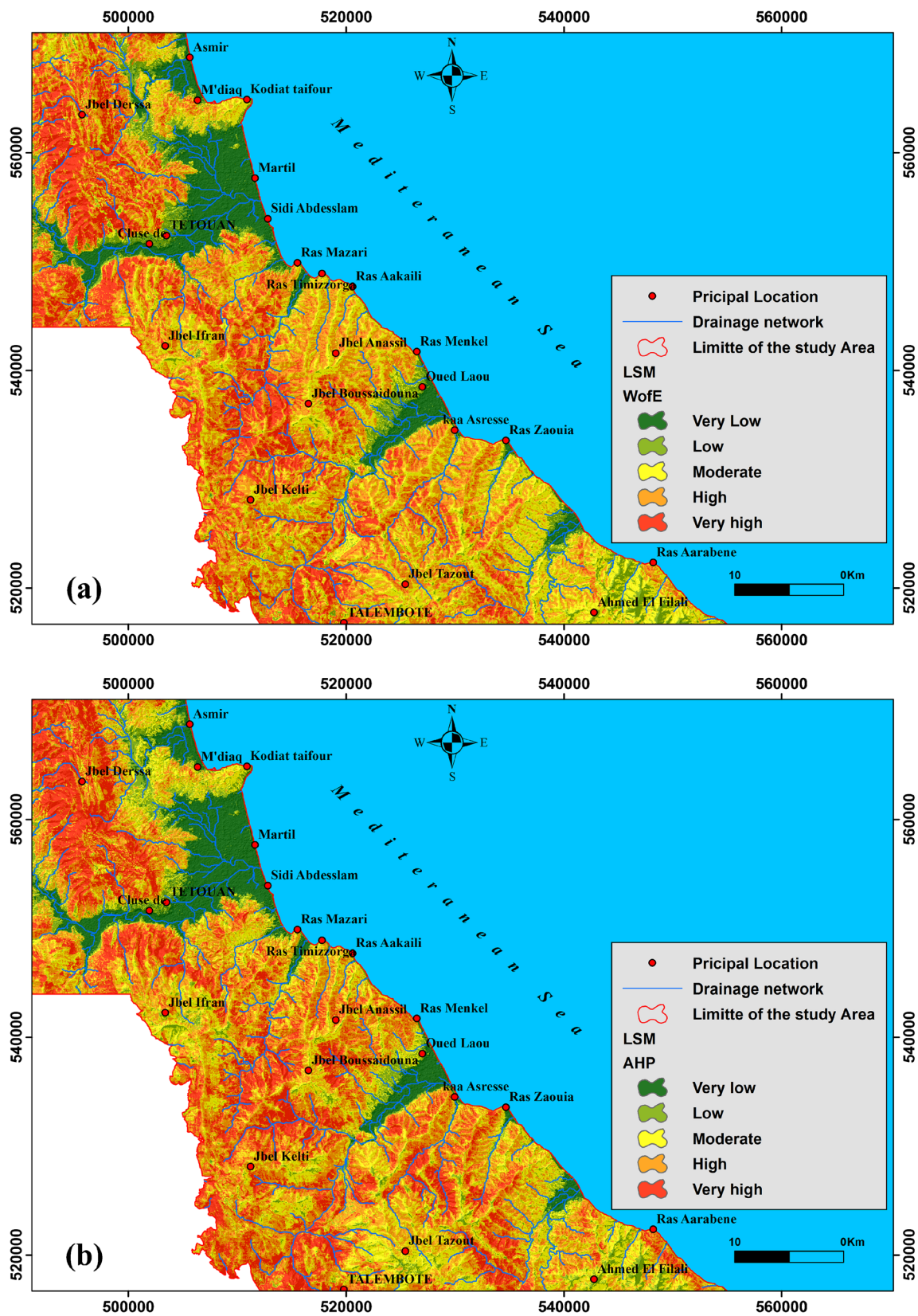


Fig. 5 Landslide susceptibility maps from a WofE and b AHP models

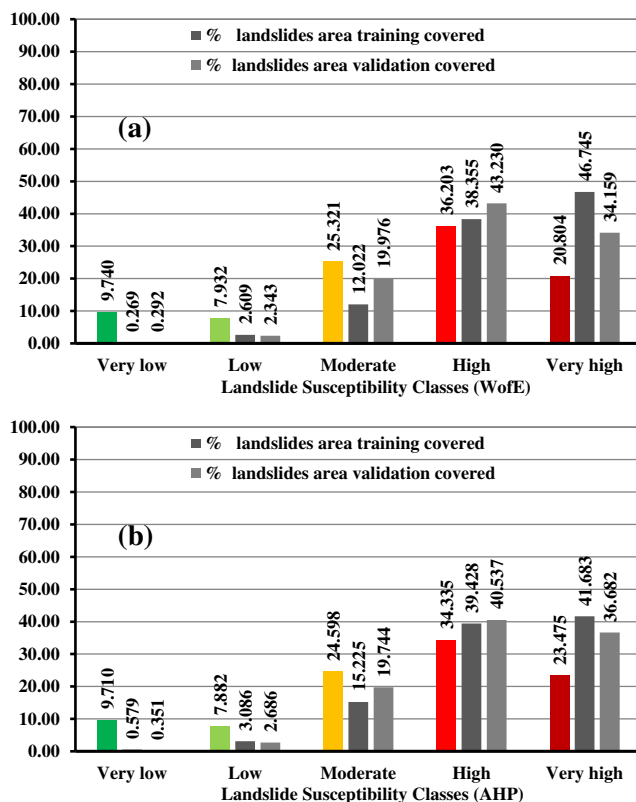


Fig. 6 Percentage of landslide susceptibility classes and landslide inventory on landslide susceptibility maps (training and validation data) for WofE (a) and AHP (b) models

$$LSM_{AHP} = \sum_{j=i}^n W_j W_{ij} \quad (7)$$

where LSM_{AHP} : landslide susceptibility map W_j : weight assigned for causative factor W_{ij} : weight assigned for the class (i) of factor (j) n : number of causative factors

Assessment and comparison of the models

The credibility and viability of any landslide susceptibility map produced according to a given model are closely dependent on both the data used and model structure. For our study, the accuracy of the prediction of two maps produced by using WofE and AHP was verified by using training landslides location and validation landslides location by applying ROC/AUC technique (Yilmaz 2010). The AUC result analyses showed that for WofE model, the success rate using training data was 77.333%, the prediction rate using validation data was 74.653 % (Fig. 7a, b), and for AHP method, the success rate and prediction rate were 72.602% and 71.394% respectively (Fig. 7a, b). According to Hong et al. (2018), a curve of a model with a largest AUC that varies from 50 to 100% can be considered the best model and consequently our results are consistent. For prediction zoning potential risk areas, the weight of evidence (WofE) method appears the most adequate

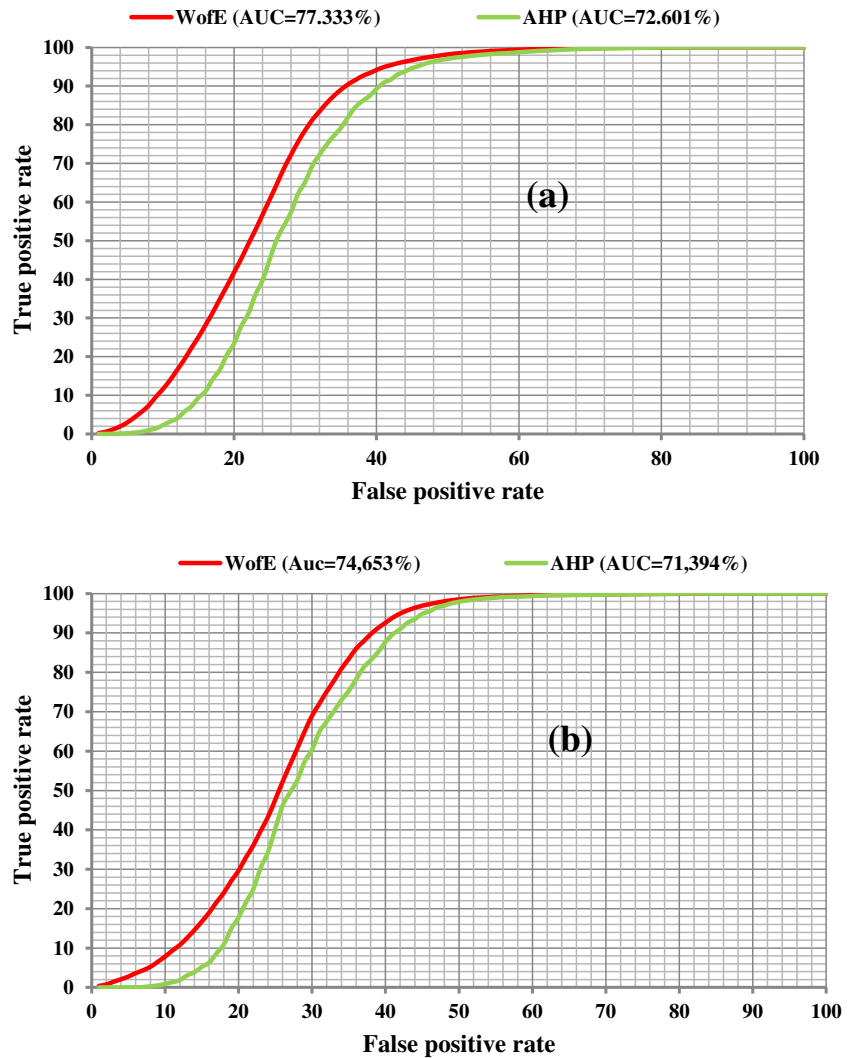
than analytic hierarchy process (AHP), according to the result of this study.

Discussion

Predicting landslide occurrence and quantifying the relationships between landslide occurrences and causative factors are often a real challenge as well as for landslide hazards and risk assessment. In this research, at the coastline between Tetouan and Bou Ahmed and its hinterlands of the Rif chain (northernmost Morocco), we combined several dataset for implanting tow models of analyses for landslide susceptibility mapping, using qualitative method (AHP) and quantitative method (WofE). The results made it possible to quantify the importance of magnitude of causative factors in landslides triggering, to understand the correlation between spatial distribution of landslides and causative factors in order to highlight the areas most exposed to landslide occurrence. According to the AHP method, elevation, slope, lithology, land use, and rainfall were respectively the most important factors followed fault proximity, stream proximity, curvature, aspect, shaded relief, and road proximity. In another research, by using AHP method and six main landslide causative factors, Brahim et al. (2018) has shown that elevation, lithology, and land use are the main factors controlling landslide occurrence at Rif scale than slope, fault density, and drainage network density. Our study adds tow causative factors important in landslide occurrence which are slope and rainfall; these findings are consistent with other studies at Rif domain which report that the main predisposing factors in landslides triggering are rainfall, lithology, elevation, slope, and land use (Millies-Lacroix 1965; Fares 1994; El Gharbaoui 1980; El Kharim 2002; El Moutchou 2014). However, to compare quantitatively the result accuracy between models, it is preferable to use similar landslide causative factors in building these models (Iqbal et al. 2021).

The mechanism of landslide occurrence is a complex and often unknown for new location; it is rarely attributed to a single causative factor (Varnes 1978; Crozier 1984; Iqbal et al. 2021). The bivariate analysis (WofE) reveals that the lowest elevations (>100m) and height elevation (>600m) show a weak influence on landslide occurrence; the superposition of these elevation classes with flat zones and the hardness of rocks of limestone ridge respectively explain widely this finding to this is added the abundant of vegetation cover and forest at high elevation, which represent an element of stability against slope failure. The middle elevation (100–600m) shows a strong impact on landslides, which characterizes the relief of Sebteide, Ghomaride nappes, flysch nappes, and Tangier unit unstable for their crushed characters. Regarding the slope impact, we expect a linear correlation between slope and landslide occurrence; however, the steepest

Fig. 7 Area under curve shows the success rate curve (a) and the predictive rate (b) of landslide susceptibility index maps, for WofE and AHP models



slope had a weak influence on landslides triggering; it corresponds to the limestone and dolomite peaks, the abrupt reliefs, and to some sandstone bars of the Flysch layers, mechanical hardness, and resistant. In terms of aspects, the North direction and West direction had the most impact on landslide occurrence as a result those directions are less exposed to solar radiation and more wetness due to the wet currents of the Mediterranean Sea and the Atlantic Ocean. The concave hillslopes had the biggest impact on landslide occurrence compared to the other geomorphology curvature. It is probably because of the topographic forms, which favoring retained rainwater under the effect of intense fracturing, the water-logged bedrock leads to significant weathering. As expected, landslide susceptibility near streams and at barren land becomes more substantial. The distance between 90 and 500m from fault is the most susceptible areas to landslides. This might be due to the disconnection created by tectonics in the soil and rocks which favoring the circulation of water and easily the triggering of landslides. In the case of the roads impact, the results showed a weak relation between landslide

occurrences and proximity to roads probably is due to the moderate number of landslide mapping alongside roads. Concerning lithofacies, the sandstones-marlstones followed by the marlstones-limestones show a strong susceptible to slope failure, overall are calcareous clays moderately plastic and weak mechanical strength. The annual rainfall factor is relevant in landslides triggering especially after heavy rainy days. The results show a correlation between rainfalls and spatial distribution of landslides except for the last three classes which exerted a weak impact; this contradiction might be due to these classes, which are superposed with the hardness of rocks of limestone and dolomite weakly sensitive to landslides and water erosion. At last, these results clearly show the close relationship between the geological, geomorphological, hydrogeological, climatic, and anthropic context on spatial distribution of landslides in the current study area, which are in agreement with the previous studies (Millies-Lacroix 1965; El Gharbaoui 1980; El Kharim 2002; El Moutchou 2014).

In this research, model validation shows satisfactory results for both methods (WofE, AHP) used in landslide

susceptibility mapping; however, WofE model was found the best model for identifying and zoning the areas more exposed to landslide occurrence, this finding is consistent with results of other literature studies (Pourghasemi et al. 2013b; Pourghasemi et al. 2013c; Nohani et al. 2019). The possibility to get better results is related to the use of other susceptibility models (Iqbal et al. 2021); this constitutes a motivation for a study under realization.

Conclusion

The coastline between Tetouan and Bou Ahmed and its hinterland subject of this study encloses several hot spots giving rise to frequent and varied landslide types, which constitute real risks on propriety, and human life is always in danger, to this is added the continuing modification of the costal and the continent landscape and consequently changing the stability of the ecosystem of these areas. For the purpose of developing and preserving these areas against landslide occurrence, landslide susceptibility map has become one of the solicited and widely proven choices worldwide in zoning areas susceptible to landslide incidence. Thus, we applied weight of evidence (WofE) and analytic hierarchy process (AHP) methods in GIS platform for producing landslide susceptibility maps.

The resulted maps showed that the area most vulnerable to the risks of landslides constitutes with approximately the same value 58% and 57% of the total of study area by WofE and AHP models, respectively. It represents approximately more than half of study area; this finding is alarming especially with the increase of unplanned housing and project development that accompanied in some case by destruction of forest and vegetation that plays an important role of stabilization of hillslope.

To perform these models, some factors such as seismicity and the variation of the piezo metric level of ground water can be added in modeling. Generally, the encouraging results obtained by WofE and AHP method showed clearly the performance of them in zoning risks within study area; it can be used at scale of belt Rif for landslide susceptibility maps or other context similar to Rif context. The results are consistent and can be used by different stakeholders especially with the development and managing that have been experienced in recent years under study area, which undoubtedly will have an impact on stability of hillslope.

Declarations

Conflict of interest The authors declare that they have no competing interest.

References

- Agliardi F, Crosta GB, Zanchi A (2001) Structural constrains on deep-seated slope deformations kinematics. *Eng Geol* 59(1-2):83–102. [https://doi.org/10.1016/S0013-7952\(00\)00066-1](https://doi.org/10.1016/S0013-7952(00)00066-1)
- Agliardi F, Crosta GB, Frattini P (2012) Slow rock slope deformation. In: Clague JJ, Stead D (eds) *Landslides types, mechanisms and modeling*. Cambridge Univ Press, Cambridge, pp 207–221
- Aleotti P, Chowdhury R (1999) Landslide hazard assessment: summary review and new perspectives. *B Eng Geol Environ* 58(1):21–44
- Althuwaynee OF, Pradhan B, Park, HJ, Lee JH (2014) A novel ensemble bivariate statistical evidential belief function with knowledge-based analytical hierarchy process and multivariate statistical logistic regression for landslide susceptibility mapping. *Catena*, 114, 21–36.
- Ayalew L, Yamagishi H (2005) The application of GIS-based logistic regression for landslide susceptibility mapping in the Kakuda-Yahiko Mountains, Central Japan. *Geomorphology* 65(1-2):15–31
- Biçer ÇT, Ercanoglu M (2020) A semi-quantitative landslide risk assessment of central Kahramanmaraş City in the Eastern Mediterranean region of Turkey. *Arab J Geosci* 13(15):1–26
- Brahim LA, Bousta M, Jemmah IA, El Hamdouni I, ElMahsani A, Abdelouafi A, Lallout I (2018) Landslide susceptibility mapping using AHP method and GIS in the peninsula of Tangier (Rif-northern morocco). In *Matec Web of Conferences* (Vol. 149, p. 02084). EDP Sciences
- Bui DT, Tuan TA, Klempe H, Pradhan B, Revhaug I (2016) Spatial prediction models for shallow landslide hazards: a comparative assessment of the efficacy of support vector machines, artificial neural networks, kernel logistic regression, and logistic model tree. *Landslides* 13(2):361–378
- Buwal B (1997) BRP: Berücksichtigung der Massenbewegungsgefahren bei raumwirksamen Tätigkeiten. Bundesamt für Umwelt, Wald und Landschaft, Bundesamt für Wasserwirtschaft, Bundesamt für Raumplanung, Bern und Biel
- Chalouan A, Galindo-Zaldívar J, Bargach K, Jabaloy A, Ahmamou M, Ruano P, Akil M (2001) Deformaciones recientes en el frente de la Cordillera Rifena (Prerif, Marruecos). *Geogaceta* 29:40–43
- Crozier MJ (1984) Field assessment of slope instability. *Slope instability*: 103–142
- Devkota KC, Regmi AD, Pourghasemi HR, Yoshida K, Pradhan B, Ryu IC, Althuwaynee OF (2013) Landslide susceptibility mapping using certainty factor, index of entropy and logistic regression models in GIS and their comparison at Mugling–Narayanghat road section in Nepal Himalaya. *Nat Hazards* 65(1):135–165
- Dramis F, Sorriso-Valvo M (1994) Deep-seated gravitational slope deformations, related landslides, and tectonics. *Eng Geol* 38(3-4):231–243
- El Gharbaoui A (1980) La terre et l’homme dans la péninsule Tingitane. Test on the man and the natural environment in Rif Western. Dr Univ of Paris-Est Créteil Val de Marne. French
- El Kharim Y (2002) Etude des mouvements de versants dans la région de Tétouan (Rif occidental): Inventaire, analyse et cartographie. These Dr es Sci Univ Abdelmalek Essaadi, Tétouan
- EL Moutchou B (2014) Caractérisation morphosédimentaire, morphodynamique, géomorphologique et dynamique des versants du littoral méditerranéen marocain entre Fnideq et Kaa Asresse (Provinces de Tétouan et Chefchaouen, Maroc Nord Occidental). Thèse d’état, UAE, Tétouan. Tétouan. 305 p
- Elmoulat M, Ait Brahim L (2018) Landslides susceptibility mapping using GIS and weights of evidence model in Tetouan-Ras-Mazari area (Northern Morocco). *Geomat Nat Haz Risk* 9(1):1306–1325
- Ercanoglu M, Gokceoglu C (2002) Assessment of landslide susceptibility for a landslide-prone area (north of Yenice, NW Turkey) by fuzzy approach. *Environ Geol* 41(6):720–730

- Fares A (1994) Essai méthodologique de la cartographie des risques naturels liés aux mouvements de terrain application à l'aménagement de la ville de Taounate (Rif, Maroc), Dr Diss, Besançon
- Flageollet JC (1989) Les mouvements de terrains et leur prévention. (éd.) Masson, série Géographie, Paris, 224 p
- Ghorbanzadeh O, Blaschke T, Gholamnia K, Meena SR, Tiede D, Aryal J (2019) Evaluation of different machine learning methods and deep-learning convolutional neural networks for landslide detection. *Remote Sens* 11(2):196. <https://doi.org/10.3390/rs11020196>
- Glade T, Crozier MJ (2005) Landslide hazard and risk: concluding comment and perspectives. *Landslide hazard and risk*. Wiley, Chichester, pp 767–774
- Goetz JN, Guthrie RH, Brenning A (2011) Integrating physical and empirical landslide susceptibility models using generalized additive models. *Geomorphology* 129(3–4):376–386
- Guzzetti F, Carrara A, Cardinali M, Reichenbach P, Galli M, Ardizzone F (1999) Landslide hazard evaluation: an aid to a sustainable development. *Geomorphology* 31(1–4):181–216
- Guzzetti F, Mondini AC, Cardinali M, Fiorucci F, Santangelo M, Chang KT (2012) Landslide inventory maps: new tools for an old problem. *Earth-Sci Rev* 112(1–2):42–66
- Hadji R, Limani Y, Baghem M, Demdoun A (2013) Geologic, topographic and climatic controls in landslide hazard assessment using GIS modeling: a case study of Souk Ahras region, NE Algeria. *Quat Int* 302:224–237
- Hamed Y, Ahmadi R, Hadji R, Mokadem N, Dhia HB, Ali W (2014) Groundwater evolution of the Continental Intercalaire aquifer of Southern Tunisia and a part of Southern Algeria: use of geochemical and isotopic indicators. *Desalin Water Treat* 52(10–12):1990–1996
- He Q, Xu Z, Li S, Li R, Zhang S, Wang N, Chen W (2019) Novel entropy and rotation forest-based credal decision tree classifier for landslide susceptibility modeling. *Entropy* 21(2):106
- Hong H, Tsangaratos P, Iliia I, Liu J, Zhu AX, Chen W (2018) Application of fuzzy weight of evidence and data mining techniques in construction of flood susceptibility map of Poyang County, China. *Sci Total Environ* 625:575–588
- Iqbal J, Cui PENG, Hussain ML, Pourghasemi HR, Cheng DQ, Shah SU, Pradhan B (2021) Landslide susceptibility assessment along the Dubair-Dudishal section of The Karakoram Highway, Northwestern Himalayas. Pakistan. *Acta Geodyn Geomater* 18(202):137–155. <https://doi.org/10.13168/AGG.2021.0010>
- Jaafari A, Panahi M, Pham BT, Shahabi H, Bui DT, Rezaie F, Lee S (2019) Meta optimization of an adaptive neuro-fuzzy inference system with grey wolf optimizer and biogeography-based optimization algorithms for spatial prediction of landslide susceptibility. *Catena* 175:430–445
- Karim Z, Hadji R, Hamed Y (2019) GIS-based approaches for the landslide susceptibility prediction in Setif Region (NE Algeria). *Geotech Geol Eng* 37(1):359–374
- Kornprobst J (1974) Contribution à l'étude pétrographique et structurale de la zone interne du Rif (Maroc Septentrional). Notes et Mémoires de la Service Géologique de Maroc, 251, 256 pp.
- Li X, Cheng X, Chen W, Chen G, Liu S (2015) Identification of forested landslides using LiDAR data, object-based image analysis, and machine learning algorithms. *Remote Sens* 7(8):9705–9726
- MATE/METL (1999) Plans de Prévention des Risques Naturels (PPR): Risques de Mouvements de Terrain, Ministère de l'Aménagement du Territoire et de l'Environnement, (MATE), Ministère de l'Équipement, des Transports et du Logement (METL), La Documentation Française, Paris.
- Millies-Lacroix A (1965) L'instabilité des versants dans le domaine rifain. *GDYAC* 15(7–8–9):97–109
- Naidu S, Sajinkumar KS, Oommen T, Anuja VJ, Samuel RA, Muraleedharan C (2018) Early warning system for shallow landslides using rainfall threshold and slope stability analysis. *Geosci Front* 9(6):1871–1882
- Nohani E, Moharrami M, Sharafi S, Khosravi K, Pradhan B, Pham BT, Melesse AM (2019) Landslide susceptibility mapping using different GIS-based bivariate models. *Water-Sui* 11(7):1402
- Oh HJ, Pradhan B (2011) Application of a neuro-fuzzy model to landslide-susceptibility mapping for shallow landslides in a tropical hilly area. *Comput Geosci* 37(9):1264–1276
- Pamela, Sadisun IA, Arifianti Y (2018) Weights of evidence method for landslide susceptibility mapping in Takengon, Central Aceh, Indonesia. *IOP Conf Ser Earth Environ Sci* 118(1)
- Park S, Choi C, Kim B, Kim J (2013) Landslide susceptibility mapping using frequency ratio, analytic hierarchy process, logistic regression, and artificial neural network methods at the Inje area, Korea. *Environ Earth Sci* 68(5):1443–1464
- Pham BT, Khosravi K, Prakash I (2017) Application and comparison of decision tree-based machine learning methods in landslide susceptibility assessment at Pauri Garhwal Area, Uttarakhand, India. *Environ Process* 4(3):711–730
- Pham BT, Bui DT, Prakash I (2018) Application of classification and regression trees for spatial prediction of rainfall-induced shallow landslides in the Uttarakhand area (India) using GIS. In *Climate change, extreme events and disaster risk reduction* (pp. 159–170). Springer, Cham
- Popesc ME (1994) A suggested method for reporting landslide causes. *Geol B Assoc Int Geol Ing* 50(1):71–74
- Pourghasemi HR, Mohammady M, Pradhan B (2012a) Landslide susceptibility mapping using index of entropy and conditional probability models in GIS: Safarood Basin, Iran. *Catena* 97:71–84
- Pourghasemi HR, Pradhan B, Gokceoglu C (2012b) Application of fuzzy logic and analytical hierarchy process (AHP) to landslide susceptibility mapping at Haraz watershed, Iran. *Nat Hazards* 63(2):965–996
- Pourghasemi HR, Moradi HR, Aghda SF (2013a) Landslide susceptibility mapping by binary logistic regression, analytical hierarchy process, and statistical index models and assessment of their performances. *Nat Hazards* 69(1):749–779
- Pourghasemi H, Pradhan B, Gokceoglu C, Moezzi KD (2013b) A comparative assessment of prediction capabilities of Dempster-Shafer and Weights-of-evidence models in landslide susceptibility mapping using GIS. *Geomat Nat Hazards Risk* 4(2):93–118
- Pourghasemi HR, Pradhan B, Gokceoglu C, Mohammadi M, Moradi HR (2013c) Application of weights-of-evidence and certainty factor models and their comparison in landslide susceptibility mapping at Haraz watershed Iran. *Arab J Geosci* 6(7):2351–2365
- Pradhan B (2010) Landslide susceptibility mapping of a catchment area using frequency ratio, fuzzy logic and multivariate logistic regression approaches. *J Indian Soc Remote Sens* 38(2):301–320
- Pradhan B (2011) Manifestation of an advanced fuzzy logic model coupled with geo-information techniques to landslide susceptibility mapping and their comparison with logistic regression modelling. *Environ Ecol Stat* 18(3):471–493
- Pradhan B (2013) A comparative study on the predictive ability of the decision tree, support vector machine and neuro-fuzzy models in landslide susceptibility mapping using GIS. *Comput Geosci* 51(1):350–365
- Pradhan B, Lee S (2010a) Regional landslide susceptibility analysis using back-propagation neural networks model at Cameron Highland, Malaysia. *Landslides* 7(1):13–30
- Pradhan B, Lee S (2010b) Delineation of landslide hazard areas on Penang Island, Malaysia, by using frequency ratio, logistic regression, and artificial neural network models. *Environ Earth Sci* 60(5):1037–1054
- Prokos H, Baba H, LóCzy D, El Kharim Y (2016) Geomorphological hazards in a Mediterranean mountain environment-example of Tétouan, Morocco. *HunGeoBull* 65(3):283–295

- Rasyid AR, Bhandary NP, Yatabe R (2016) Performance of frequency ratio and logistic regression model in creating GIS based landslides susceptibility map at Lompobattang Mountain, Indonesia. *Geoenviron Disasters* 3(1):19
- Regmi NR, Giardino JR, Vite JD (2010) Modeling susceptibility to landslides using the weight of evidence approach: Western Colorado, USA. *Geomorphology* 115(1-2):172–187
- Regmi AD, Devkota KC, Yoshida K, Pradhan B, Pourghasemi HR, Kumamoto AA (2014) Application of frequency ratio, statistical index, and weights-of-evidence models and their comparison in landslide susceptibility mapping in Central Nepal Himalaya. *Arab J Geosci* 7(2):725–742
- Reichenbach P, Rossi M, Malamud BD, Mihir M, Guzzetti F (2018) A review of statistically-based landslide susceptibility models. *Earth Sci Rev* 180:60–91
- Saaty TL (1980) The analytical hierarchy process, planning, priority. Resource allocation. RWS publications, USA
- Saha S, Saha A, Hembram TK, Pradhan B, Alamri AM (2020) Evaluating the performance of individual and novel ensemble of machine learning and statistical models for landslide susceptibility assessment at Rudraprayag District of Garhwal Himalaya. *Appl Sci* 10(11):3772
- Sidle RC, Ochiai H (2007) Landslides processes, prediction, and land use water resources monograph 18. *Natural Resources Forum* 31:322–326
- Song KY, Oh HJ, Choi J, Park I, Lee C, Lee S (2012) Prediction of landslides using ASTER imagery and data mining models. *Adv Space Res* 49(5):978–993
- Thapa D, Bhandari BP (2019) GIS-based frequency ratio method for identification of potential landslide susceptible area in the Siwalik Zone of Chatara-Barahakshetra Section, Nepal. *Open J of Geol* 9(12):873–896
- Van Den Eeckhaut M, Vanwalleghem T, Poesen J, Govers G, Verstraeten G, Vandekerckhove L (2006) Prediction of landslide susceptibility using rare events logistic regression: a case-study in the Flemish Ardennes (Belgium). *Geomorphology* 76(3-4):392–410
- Van Den Eeckhaut M, Kerle N, Poesen J, Hervás J (2012) Object-oriented identification of forested landslides with derivatives of single pulse LiDAR data. *Geomorphology* 173:30–42
- Van Westen CJ (2000) The modelling of landslide hazards using GIS. *Surv Geophys* 21(2-3):241–255
- Van Westen CJ, Van Asch TW, Soeters R (2006) Landslide hazard and risk zonation—why is it still so difficult? *B Eng geol Environ* 65(2): 167–184
- Varnes DJ (1978) Slope movement types and processes. Special Report 176:11–33
- Voogd H (1983) Evaluation multicritère pour la planification urbaine et régionale. Londres: Pion.
- Wildi W (1983) La chaîne tello-rifaine (Algérie, Maroc, Tunisie): structure, stratigraphie et évolution du Trias au Miocène. *Rev Geogr Phys Geol* 24(3):201–297
- Wu Z, Wu Y, Yang Y, Chen F, Zhang N, Ke Y, Li W (2017) A comparative study on the landslide susceptibility mapping using logistic regression and statistical index models. *Arab J Geosci* 10(8):187
- Yalcin A, Reis S, Aydinoglu AC, Yomralioglu T (2011) A GIS-based comparative study of frequency ratio, analytical hierarchy process, bivariate statistics and logistics regression methods for landslide susceptibility mapping in Trabzon, NE Turkey. *Catena* 85(3):274–287
- Yilmaz I (2010) Comparison of landslide susceptibility mapping methodologies for Koyulhisar, Turkey: conditional probability, logistic regression, artificial neural networks, and support vector machine. *Earth Environ Sci* 61(4):821–836
- Zhang W, Goh AT, Zhang Y, Chen Y, Xiao Y (2015) Assessment of soil liquefaction based on capacity energy concept and multivariate adaptive regression splines. *Eng Geol* 188:29–37
- Zorn M, Komac B (2007) Probability modelling of landslide hazard. *Acta Geogr Slov* 47(2):139–169